degree 2 for the H's and degree 1 for the s's.

$$H_\rho = \mu_{\rho 0} + \mu_{\rho 1} r_k + \mu_{\rho 2} r_k^2 + \mu_{\rho 3} \varphi_k + \mu_{\rho 4} \varphi_k^2 \quad (5a)$$

$$H_\tau = \mu_{\tau 0} + \mu_{\tau 1} r_k + \mu_{\tau 2} r_k^2 + \mu_{\tau 3} \varphi_k + \mu_{\tau 4} \varphi_k^2 \quad (5b)$$

$$s\rho = \nu_{\rho 0} + \nu_{\rho 1} r_k + \nu_{\rho 2} \varphi_k \quad (5c)$$

$$s_\tau = \nu_{\tau 0} + \nu_{\tau 1} r_k + \nu_{\tau 2} \varphi_k \quad (5d)$$

The regression for H parameters was performed twice by considering, alternatively, the values $H_\rho^\bullet$ and $H_\tau^\bullet$ obtained with the $s = 2$ condition imposed and the values H_ρ and H_τ obtained with the latter condition waived. The "best" μ and ν coefficients were determined by using again the least-square approach minimizing the sum $\sum(Y_{obsd} - Y_{calcd})^2$ ($Y = H$ or s) for the 28 observations listed in Table I (the last five regressions give two observations each). In each case it was considered the root-mean-square deviation S and the overall index of correlation R[11] (see Table II). From the results it is evident that the standard errors for μ and ν parameters based on the above regression formula are very high. So we have tried other regressions, also listed in Table II, with lesser parameters and found that H_ρ and H_τ can be expressed satisfactorily by $3 + 3$ μ values instead $5 + 5$ while $H_\rho^\bullet$ and $H_\tau^\bullet$ are not expressed as well (especially $H_\tau^\bullet$). The regression of s_ρ and s_τ (especially s_ρ) gives instead a weak dependence both on r_k and on φ_k suggesting the use of constant s values or, possibly, s_ρ constant and s_τ a linearly variable with r_k only. Furthermore only s_τ differs appreciably from 2, and also along τ the use of an $s \neq 2$ value gives only a modest improvement.

Conclusion

The present analysis has confirmed also for PIB diffraction spectra the feasibility of Gauss functions both for expressing the intensity distribution functions along constant-2ϑ lines and along variable-2ϑ lines. Statistical coefficients of regression have also shown that the dependence of peak widths on film position is close to a bilinear relationship against the polar coordinates of the peak.

In the following paper we shall report how—on the basis of this analysis—a structure refinement of PIB was performed by using the whole fiber diffraction pattern. We shall also discuss the importance of combining the whole-pattern approach with constrained refinement.

Acknowledgment. We are indebted to Prof. G. Zannotti, Università di Padova, for the use of Optronics photoscan instrument and for useful discussions. Financial support by Ministero della Pubblica Istruzione and Consiglio Nazionale delle Ricerche is also acknowledged.

Registry No. PIB, 9003-27-4.

References and Notes

(1) Immirzi, A.; Iannelli, P. *Gazz. Chim. Ital.* **1987**, *117*, 201.
(2) Immirzi, A.; Iannelli, P. *Macromolecules* **1988**, *21*, 768.
(3) Rietveld, H. M. *Acta Crystallogr.* **1967**, *22*, 151.
(4) Rietveld, H. M. *J. Appl. Crystallogr.* **1969**, *2*, 65.
(5) Tanaka, T.; Chatani, Y.; Tadokoro, H. *J. Polym. Sci., Polym. Phys. Ed.* **1974**, *12*, 515.
(6) Iannelli, P.; Immirzi, A. *Acta Crystallogr. Sect. A: Found Crystallogr.* **1987**, *A43*, C-199.
(7) Iannelli, P.; Immirzi, A. *Macromolecules*, following paper in this issue.
(8) Hall, M. M., Jr.; Veeraraghavan, V. G.; Rubin, H.; Winchell, P. G. *J. Appl. Crystallogr.* **1977**, *10*, 66.
(9) Ortega, J. M.; Reinholdt, W. C. *Iterative Solution of Nonlinear Equations in Several Variables*; Academic: New York, 1970.
(10) Millane, R. P.; Arnott, S. *J. Macromol. Sci., Phys.* **1985**, *B24*, 193.
(11) Wheaterburn, C. E. *A First Course in Mathematical Statistics*; Cambridge University: New York, 1977.

Structure Analysis of Polyisobutylene Based on the Whole-Pattern Fiber Diffraction Method. 2. Refinement of Structure Based on Several Constrained Models

Pio Iannelli and Attilio Immirzi*

Dipartimento di Fisica, Università di Salerno, I-84100 Salerno, Italy.
Received January 6, 1988; Revised Manuscript Received June 8, 1988

ABSTRACT: On the basis of the results of a spot-by-spot analysis of the X-ray fiber diffraction pattern of polyisobutylene the structure of this polymer has been refined according to the "whole-pattern" approach. The starting point was the structure by Tadokoro and the method used was that of "constrained refinement" considering fixed C–C bond lengths and free bond and torsion angles. It is shown that the whole-pattern approach is a practical tool for refining structures of fibrous materials also in cases of considerable structural complexity provided the number of unknowns is properly reduced. By assuming that all CMe_2–CH_2–CMe_2 chain bond angles are equal to each other as well as CH_2–CMe_2–CH_2 angles, one obtains the values 129° and 110° for the above bond angles with the eight chain torsional angles −48°, −168°, −60°, −157°, −54°, −167°, −54°, and −166°, in excellent agreement with previously obtained values.

Introduction

Structure refinement of crystalline fibrous materials can be undertaken, as discussed in the preceding paper,[1] by using the "whole-pattern" instead of "integrated" intensities. By using an empirical approach we have obtained for polyisobutylene (PIB) crystallized under stretching a number of peak parameters which allow for reproducing with sufficient accuracy the effective intensity distribution function (idf) for the X-ray diffraction pattern. On this basis the crystal structure can be refined by optimizing *both* structural parameters and peak parameters.

The whole-pattern approach, based on a least-square fitting procedure, has been outlined in previous papers.[2,3] The fit is performed by comparing the "observed" diffraction intensities $I_{obsd,i}$ with the ones calculated as $S\sum_k I_k \Omega_{ik}$ where S denotes a scale factor, i any measured

0024-9297/89/2222-0200$01.50/0

point of the diffraction pattern, k any Bragg reflection, I_k the corresponding "calculated" integrated intensity, and Ω_{ik} a normalized two-variable intensity distribution function expressed in a proper parametrized form. The I_k values depend on "structure" (atomic coordinates and thermal parameters) through the relationship

$$I_k = m_k L_k p_k F_k^2 \quad (1)$$

where F_k is the structure factor of the kth reflection and m_k, L_k, and p_k are the multiplicity, Lorentz, and polarization factors. The Ω_{ik} function has the form widely discussed in the previous paper[1] and depends on instrumental quantities, on lattice constants, and on morphological parameters.

As the observed $I_{obsd,i}$ are measured on several films, an equal number of scale factors must be considered. By addition also of a contribution $B_{calcd,i}$ for diffuse diffraction (background) expressed by a parametrized function and introduction of statistical weight factors for taking into account the variability of standard errors of the measurements ($w_i = 1/\sigma_i^2$), the minimized function is

$$\chi^2 = \sum_i w_i[I_{obsd,i} - S_{n_i}(B_{calcd,i} + \sum_k I_k \Omega_{ik})]^2 \quad (2)$$

where n_i is the film to which the ith observation belongs.

Owing to the limited information contained in the fiber spectrum, structure refinement of fibrous materials must be necessarily carried out by means of "constrained refinement"[4] taking into account all a priori structural information available with accuracy higher than that expected from the refinement itself (e.g., bond angles, planarity of groups, etc.). This will be accomplished by the use of "internal" coordinates (ic) rather than the usual atomic fractional coordinates. In addition it is often necessary to impose some constraining condition which ensure the chain continuity[6] and refinement must be performed by using Lagrange multipliers.

Structure Refinement of Polyisobutylene

The structure of PIB has been an intriguing problem for a long time and several models were proposed, based on regular helices, until Tadokoro et al.[5] succeeded in finding the correct solution, forsaking the assumption of a regular helix structure. According to these authors the space group is $P2_12_12_1$ with 16 $-CH_2C(CH_3)_2-$ chemical units per unit cell; the chain has 2_1 screw symmetry and the conformation of the four C_4H_8 units constituting the crystallographic asymmetric unit are different from each other.

We have based our work on Tadokoro's model considering as a starting point for the refinement Tadokoro's structure also varying at random some parameters (see below). In view of doing constrained refinement we have considered (see Figure 1) the following internal coordinates: (i) eight C–C chain bond lengths (bl) l_1, l_2, ..., l_8; (ii) one C–C side bl l_s, relative to *all* C–CH_3 bonds; (iii) eight chain bond angles (ba) ϑ_1, ϑ_2, ..., ϑ_8, of which the odd values refer to CH_2–C–CH_2 angles and the even values to C–CH_2–C angles; (iv) eight chain torsion angles ψ_1, ψ_2, ..., ψ_8; (v) four groups of 4 × 4 bond angles ϑ_{ik} defined in Figure 1, which refer (i = 2,4,6,8) to the four quaternary C atoms; (vi) two overall rotation Φ and translation z_0 parameters.

The crystallographic structure can easily be calculated as a function of the above 43 ic. The degree of freedom (df) is really lower since the C'_1 atom (see Figure 1) must coincide with the C_1 atom operated by a 2_1 screw axis (chain continuity) and this implies three "constraints" which reduce the df to 40.

Several models have decidedly lower df can be easily treated either by keeping some ic fixed or by imposing

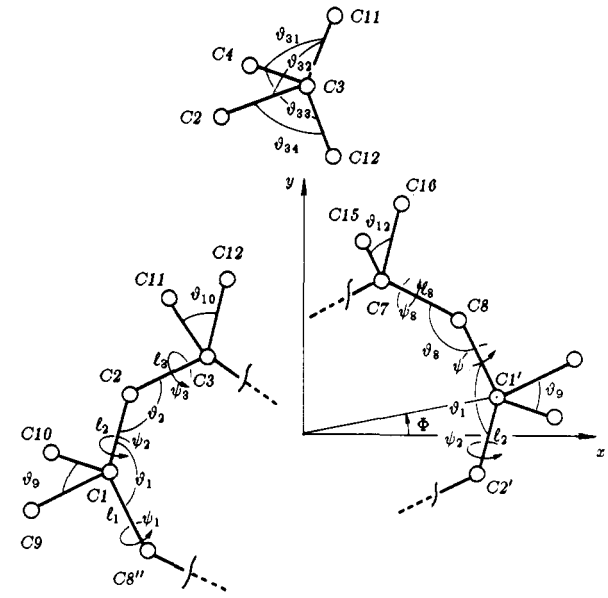

Figure 1. Internal coordinates for defining the crystal structure of PIB (arbitrary conformation). The atom labeling is also indicated.

simple relationships among internal coordinates. The first reduction of df from 40 to 31 is accomplished by assuming *fixed and known bond lengths* (bl are certainly known a priori with accuracy higher than that expected). Further reductions are suggested by chemical evidence: (i) the equivalence of the chemically omologous chain ba (*not* of the torsion angles as the chain possess irregular conformation!), implying the conditions $\vartheta_1 = \vartheta_3 = \vartheta_5 = \vartheta_7$ and $\vartheta_2 = \vartheta_4 = \vartheta_6 = \vartheta_8$; (ii) the structural equivalence of the four quarternary C atoms, implying the conditions $\vartheta_{2k} = \vartheta_{4k} = \vartheta_{6k} = \vartheta_{8k}$ for each k = 1,2,3,4; (iii) the possible *local* symmetry of the four bonds coming out from the above C atoms; the latter implies for i = 1,3,5,7 the condition $\vartheta_{i1} = \vartheta_{i2} = \vartheta_{i3} = \vartheta_{i4}$ (C_{2v} symmetry), or $\vartheta_{i1} = \vartheta_{i4}$ and $\vartheta_{i2} = \vartheta_{i3}$ (C_2 symmetry), or $\vartheta_{i1} = \vartheta_{i3}$ and $\vartheta_{i2} = \vartheta_{i4}$ (C_s symmetry, mirror plane containing the chain), or $\vartheta_{i1} = \vartheta_{i2}$ and $\vartheta_{i3} = \vartheta_{i4}$ (C'_s symmetry, mirror plane containing the two CH_3 groups).

Calculation and Results

Data used for the structural analysis are those of the preceding work.[1] The starting values for ϑ_i, ψ_i, Ψ, and z_0 parameters where evaluated from the atomic coordinates by Tadokoro[5] by using the condition of identical homologous ba and the local C_{2v} symmetry for the chain atoms bonded to methyl groups. Keeping structural parameters fixed, we have then ajusted the nonstructural quantities with the following procedure:

(1) For the calculation of $I_{calcd,i}$ the working formulas are (1) of this paper and (1)–(3) of the preceding paper (see also ref 2). The ls refinement was also that described in ref 3. In addition, Lagrange multipliers were introduced for accounting for the chain continuity according to ref 6.

(2) Lattice constants were kept fixed to Tadokoro's values. To account for film-shrinkage effects, however, the camera radius R_c (nominally 28.65 mm) was refined.

(3) Scale factors S_i were initially constrained to vary proportionally to film exposures and subsequently released as independent quantities.

(4) The isotropic thermal vibration with a unique B_{iso} according to the factor $\exp(-B_{iso} \sin^2 \vartheta/\lambda^2)$ was considered.

(5) The noncrystalline fraction of PIB (which is modest) is clearly nonoriented and the fiber spectrum displays a single uniform broad "ring" at $2\vartheta \approx 14.6°$. The background

Table I
Nonstructural Parameters at the End of the 13-Parameter Refinement[a]

effective film bending radius	R_c = 28.45 (3) mm
half-height width along ρ according to $H_\rho = H_\rho^0 + \mu_{\rho 1} r_k + \mu_{\rho 3}\varphi_k$	H_ρ^0 = 0.324 (9) mm $\mu_{\rho 1}$ = 0.0223 (6) $\mu_{\rho 3}$ = 0.109 (5) mm/rad
half-height width along τ according to $H_\tau = H_\tau^0 + \mu_{\tau 1} r_k + \mu_{\tau 3}\varphi_k$	H_τ^0 = 0.35 (2) mm $\mu_{\tau 1}$ = 0.092 (1) $\mu_{\tau 3}$ = −0.02 (1) mm/rad
film scale factors (conversion from [electron/cell]^2 intensities to arbitrary units)	S_1 = 0.026 30 (4) S_2 = 0.0994 (1) S_3 = 1.040 (2) S_4 = 1.991 (3)
background parameters according to $B_{calcd,i} = (b_1/b_2)\exp[-((\rho - \rho_0)/b_2)^2] + b_3 + b_4 \sin\vartheta$	b_3 = 95.5 (4) b_4 = −140 (1) b_1 = 364 (2) b_2 = 1.94 (1) ρ_0 = 7.29 (1)

[a] C_{2v} symmetry for all quaternary C atoms and equivalent monomeric units.

intensity (see also ref 1) was so considered, expressed by the empirical parametrized formula

$$B_{calcd,i} = B_{halo} + b_3 + b_4 \sin\vartheta$$

where B_{halo} was expressed by means of a Gaussian formula:

$$B_{halo} = \frac{b_1}{b_2}\exp\left[-\left(\frac{\rho - \rho_0}{b_2}\right)^2\right]$$

(6) On the basis of the preceding analysis, Gauss functions were used for profile function along both τ-lines and ρ-lines. Peak widths H_ρ and H_τ were assumed to vary with the polar coordinates of the spot on the film r_k, φ_k according to the bilinear relationship

$$H_\rho = H_\rho^0 + \mu_{\rho 1} r_k + \mu_{\rho 3}\varphi_k$$

$$H_\tau = H_\tau^0 + \mu_{\tau 1} r_k + \mu_{\tau 3}\varphi_k$$

All the above quantities, set initially to the values coming from the preceding analysis,[1] were refined together with the structural variables.

First we have considered the model with the least df (13 structural variables). The result was a fast convergence to the values listed in Table I and Table II, column B. The corresponding atomic fractional coordinates are listed in Table III and the molculer model is shown in Figure 2. Figure 3 shows the graphical comparison between observed and calculated intensities at the convergence point. Figure 4 displays the calculated diffraction pattern.

The results were compared with the ones by Tadokoro[5] (subsequently termed "previous" values) and with the value expected from the sp^3 hybridization geometry. The chain conformations (see the eight ψ_i values in Table II, column B) are in close agreement with the previous ones (column A) with differences ranging 1–8° with a mean of 3° (Tadokoro claims a larger average standard error for ψ's, viz., 6°). The four C–CH_2–C chain angles (imposed equal) are 129° compared to the previous 130°, 129°, 128°, and 127°. The large deviation from the canonical 109.5° value, which occur also in low molecular weight model compound such as 2,2,4,4-tetramethyladipic acid,[7] is so confirmed. The four CH_2–C–CH_2 chain angles (imposed equal) are 110° compared to the previous 110°, 109°, 112°, and 109°. The 16 side ba CH_2–C–CH_3 (equal to each other within the C_{2v} symmetry) are 109°, while the previous (calculated from the published atomic coordinates) values are in the range 107–109°. Some perplexity remains instead for the 103° value resulting for the CH_3–C–CH_3 angle, rather different indeed from the regular 109.5°. We

Table II
Structural Parameters Resulting from the Various Refinements Performed[a]

	Tadokoro value	constrained ϑ_i					independent	constrained ϑ_i,
	A	B	C	D	E	F	ϑ_i; G	constrained ψ_i; H
symm of quat C		C_{2v}	C_2	C_s	C_s'	E	C_{2v}	C_{2v}
no. of variables		13	14	14	14	16	19	7
ϑ_1	109°	109.9 (1)°	110.5 (1)°	109.4 (1)°	110.5 (1)°	110.6 (1)°	108.0 (5°)	110.2 (2)°
ϑ_3	112°	109.9 (1)°	110.5 (1)°	109.4 (1)°	110.5 (1)°	110.6 (1)°	115.2 (4)°	110.2 (2)°
ϑ_5	109°	109.9 (1)°	110.5 (1)°	109.4 (1)°	110.5 (1)°	110.6 (1)°	113.5 (4)°	110.2 (2)°
ϑ_7	110°	109.9 (1)°	110.5 (1)°	109.4 (1)°	110.5 (1)°	110.6 (1)°	101.2 (4°)	110.2 (2)°
ϑ_2	130°	129.2 (2)°	127.2 (1)°	129.9 (2)°	127.2 (1)°	126.7 (1)°	132.8 (3)°	128.9 (10)°
ϑ_4	129°	129.2 (2)°	127.2 (1)°	129.9 (2)°	127.2 (1)°	126.7 (1)°	130.6 (4)°	128.9 (10)°
ϑ_6	128°	129.2 (2)°	127.2 (1)°	129.9 (2)°	127.2 (1)°	126.7 (1)°	119.4 (3)°	128.9 (10)°
ϑ_8	127°	129.2 (2)°	127.2 (1)°	129.9 (2)°	127.2 (1)°	126.7 (1)°	139.7 (5)°	128.9 (10)°
ψ_1	47°	48.4 (2)°	47.0 (2)°	47.9 (1)°	51.3 (2)°	49.8 (2)°	58.8 (4)°	53.2 (1)°
ψ_2	167°	167.7 (2)°	165.1 (6)°	167.4 (6)°	164.3 (3)°	163.4 (3)°	158.7 (3)°	166.8 (2)°
ψ_3	51°	60.0 (2)°	61.3 (2)°	59.9 (2)°	59.9 (2)°	60.9 (2)°	54.8 (4)°	53.2 (1)°
ψ_4	160°	156.4 (2)°	154.3 (2)°	156.4 (1)°	154.5 (1)°	153.4 (2)°	157.7 (4)°	166.8 (2)°
ψ_5	55°	53.7 (2)°	54.7 (2)°	54.5 (2)°	55.6 (2)°	55.6 (2)°	59.6 (4)°	53.2 (1)°
ψ_6	167°	166.7 (2)°	164.1 (1)°	166.3 (2)°	164.1 (2)°	163.1 (2)°	172.5 (4)°	166.8 (2)°
ψ_7	62°	54.9 (2)°	53.4 (2)°	55.0 (2)°	56.9 (2)°	55.8 (2)°	37.1 (3)°	53.2 (1)°
ψ_8	165°, 165.5 (2)°	163.6 (3)°	165.0 (2)°	162.9 (2)°	162.0 (2)°	175.7 (4)°	166.8 (2)°	53.2 (1)°
ϑ_{i1}	106°, 110°, 112°, 108°	110.7 (1)°	109.1 (1)°	109.6 (1)°	113.6 (1)°	111.6 (2)°	110.9 (2)°	110.9 (1)°
ϑ_{i2}	114°, 109°, 109°, 111°	110.7 (1)°	112.6 (1)°	112.1 (1)°	113.6 (1)°	114.4 (2)°	109.0 (3)°	110.9 (1)°
ϑ_{i3}	110°, 110°, 110°, 111°	110.7 (1)°	112.6 (1)°	109.6 (1)°	108.2 (1)°	109.7 (2)°	109.5 (3)°	110.9 (1)°
ϑ_{i4}	109°, 109°, 107°, 108°	110.7 (1)°	109.1 (1)°	112.1 (1)°	108.2 (1)°	108.2 (2)°	112.7 (3)°	110.9 (1)°
Ψ	−33°	−36.1 (2)°	−36.9 (3)°	−37.2 (3)°	−38.9 (3)°	−38.8 (3)°	−31.7 (3)°	−34.5 (1)°
z_0	0.88 Å	0.873 (2) Å	0.881 (2) Å	0.900 (4) Å	0.879 (2) Å	0.893 (4) Å	0.845 (3) Å	0.987 (2) Å
ϑ_{met}	107°, 108°, 109°, 108°	103.9°	102.8°	103.9°	102.2°	101.9°	105.1°	102.8°
R_1		0.059	0.058	0.057	0.057	0.058	0.060	0.057
R_2		0.106	0.105	0.106	0.106	0.105	0.107	0.110
R_3		0.056	0.057	0.056	0.056	0.057	0.058	0.061
R_4		0.059	0.059	0.059	0.059	0.058	0.056	0.063

[a] The nonstructural parameters were refined only in the B case. The standard errors indicated in parentheses are those resulting from the diagonal terms of the inverted normal matrix and are, possibly, underestimated. C–C bond lengths were fixed to 1.540 Å. The combination of hydrogen atoms was included on the basis of the atomic positions calculated according to sp^3 geometry and assuming staggered conformations for the methyl groups. $R_1 \ldots R_4$ are the R-indices $\sum|I_{obsd,i} - I_{calcd,i}|/\sum I_{obsd,i}$ evaluated for the four films separately. ϑ_{met} is the common value for the CH_3–C–CH_3 bond angle.

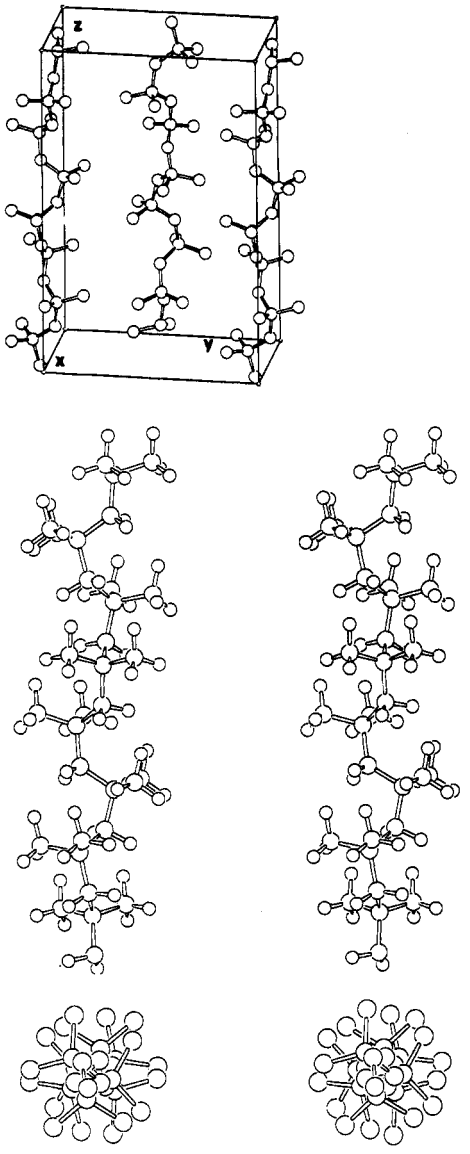

Figure 2. (Top) A perspective view of one-half unit cell of PIB ($0 \leq x \leq {}^1/_2$) is shown; the structure is that corresponding to refinement B (constrained ϑ_i and C_{2v} symmetry); hydrogen atoms are omitted. (Bottom left) Molecular model for a single chain of PIB as resulting from refinement B. (Bottom right) As above for refinement H (4_3 helix).

Table III
Atomic Fractional Coordinates Corresponding to Refinement B[a]

atom	x/a	y/b	z/c
C(1)	0.3570 (10)	0.0451 (5)	0.0470 (1)
C(2)	0.3419 (10)	0.0287 (5)	0.1290 (1)
C(3)	0.1591 (11)	0.0187 (12)	0.1763 (2)
C(4)	0.2153 (11)	0.0286 (8)	0.2562 (2)
C(5)	0.3541 (15)	−0.0451 (9)	0.3008 (3)
C(6)	0.3041 (13)	−0.0353 (8)	0.3813 (2)
C(7)	0.2848 (19)	0.0707 (8)	0.4282 (3)
C(8)	0.2789 (16)	0.0379 (8)	0.5082 (2)
C(9)	0.3069 (26)	0.1668 (5)	0.0261 (3)
C(10)	0.5686 (11)	0.0305 (16)	0.0216 (3)
C(11)	0.0529 (28)	−0.0928 (19)	0.1619 (4)
C(12)	0.0086 (20)	0.1089 (23)	0.1559 (4)
C(13)	0.5672 (11)	−0.0117 (21)	0.2871 (4)
C(14)	0.3440 (39)	−0.1683 (8)	0.2760 (4)
C(15)	0.1019 (30)	0.1378 (10)	0.4073 (4)
C(16)	0.4531 (33)	0.1527 (16)	0.4134 (4)

[a] Standard errors are in parentheses.

point out, however, that the latter result may be merely a consequence of libration effects in the side groups as discussed by Johnson.[8] Besides authentic "thermal effects" conformational disorder can also play a role.

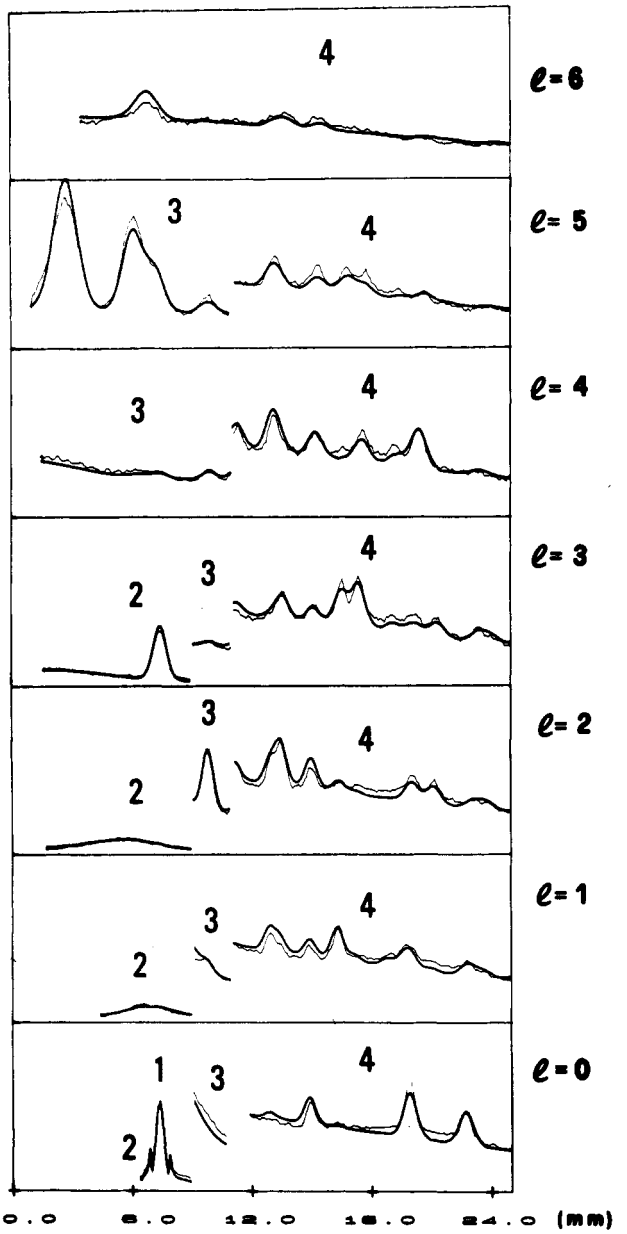

Figure 3. Comparison of observed (thin lines) and calculated (thick lines) diffracted intensities at the end of refinement B. The plots refer to sections along the layer lines of the diffraction pattern (y, mm; l = 0, 1, ..., 6, as indicated). Diffracted intensities are plotted in arbitrary units and the film number is also indicated.

We have then performed more refinement runs increasing the df of the model with the purpose of verifying if, gradually waiving the structural constraints, the reliability of results is improved or becomes worse. To this end we have taken 2 approaches: (i) to waive the condition of local C_{2v} symmetry for each quaternary carbon atom; (ii) to waive the condition of equivalence among the four quaternary carbon atoms.

According to the first line we have considered, alternatively, the local symmetries C_2, C_s (mirror symmetry in the plane of the chain), C'_s (mirror symmetry in the CH_3–C–CH_3 plane), and E (no symmetry). The results of these four trials are given in Table II. There are clearly only small differences with respect to the most constrained C_{2v} model: a little improvement in the C_s case and a little worsening in the other cases.

According to the second line we have first done refinement runs based on the C_{2v} symmetry model with distinct

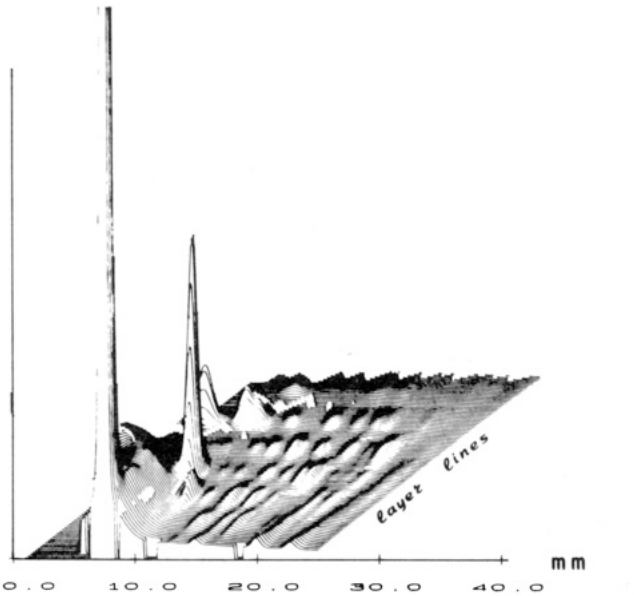

Figure 4. 3D plot of the calculated diffraction pattern showing the continuous character of the function.

ϑ for the four quaternary carbon atoms and then considered the less symmetrical C_2, C_s, C'_s, and E models with distinct parameters for the four monomeric units. The first of these trials gave the parameters listed also in Table II (column G) which appear decidedly less reliable. The other trials, though convergence is always fulfilled, gave in all cases some valence angles less than 100°; these values were unreliable so that we did not believe they merit publication.

Another refinement run was lastly performed (see column H) according to a still more symmetrical model: the regular 8_3 helix, corresponding to the model proposed by Allegra et al.[9] This seven-variable model, treated as that of column B with the additional conditions $\psi_1 = \psi_3 = \psi_5 = \psi_7$ and $\psi_2 = \psi_4 = \psi_6 = \psi_8$, give also convergence. The agreement R indices are really little higher than in B case, but the fit appears worst in specific regions of the spectrum, viz., near the (122) reflection (film no. 3). If refined atomic positions are compared, one observes, however, that the distortion from 8_3 symmetry assessed by Tadokoro is indeed modest (the rms displacement between the corresponding atoms is 0.21 Å, the largest displacement is 0.31 Å). Truly the diagnosis of distortion on the basis of a single overall index of agreement appears problematic and it is better to base oneself on the examination of specific regions of the spectrum. The determination of more reliable profile functions would surely improve the observed-to-calculated fit and allow more meaningful agreement indices.

We have finally considered an important aspect of the whole-pattern method, i.e., the ability to find a unique convergence point starting from coarse models. To this end the 13-variable model (column B) was considered and the starting parameters were modified at random by increasing amounts (but complying the chain continuity condition). As Table IV shows, the ls procedure converges *always to the same structure*, even when initial parameters are considerably modified.

Conclusions

This work has not really given substantial novelties about PIB's structure, barring that the distortion of the 8_3 helix symmetry assessed by Tadokoro (and anyhow modest) seems less evident considering the overall agreement index of the whole-pattern fit. The important result instead is that we have proved, also in a case of considerable complexity, that the "whole-pattern" approach to the refinement of fibrous structure is a practical tool *also with a coarse initial model*. It has been also proved that it is of critical importance to reduce the degree of freedom of structural models used in order to obtain meaningful results.

Table IV
Test of Convergency[a]

d_{av}				
0.57, test 1	0.73, test 2	0.82, test 3	0.84, test 4	convergence angles
Initial Chain Torsion Angles				
48	32	46	63	47.8
172	165	178	178	168.2
54	71	68	60	60.4
153	172	157	173	156.2
50	42	57	70	53.9
158	169	162	179	166.3
47	70	45	38	54.7
166	157	163	174	165.3
Initial Bond Angles				
105	113	112	103	103.9
102	126	104	104	109.9
123	126	140	127	129.1

[a] Some of the tests are given. d_{av} indicates for each test the root-mean-square deviation of atomic positions of the starting model with respect to the "true" model.

The comparison between results of a traditional analysis based on integrated intensities and those of a full-pattern analysis remains, in the case of fibers, problematical such as in the Rietveld analysis of powders,[10] with the aggravating circumstance that with fibrous polymers reliable measurements of integrated intensities are rare and "traditional" structure refinements are not a firm reference as analyses based on single-crystal technique are.

The standard errors estimated through the ls procedure (see the values published) are indeed altered because the "observations" near each other in the spectrum are anything but uncorrelated.[10] The true "number of observations" is certainly less than the number of sampled points when the resolution is, say, 100 × 100 μm.

The observations by Cooper[11] that it is desirable to distinguish structural parameters (controlling intensity) and unit-cell and profile parameters (controlling positions in the diffraction pattern) are certainly applicable also to this two-dimensional variant of the Rietveld method. The extension from the powder case and neutron diffraction to fibrous polymers and X-ray diffraction is not, however, a simple matter, owing to the severe overlap present in our case, and it is evident that this matter deserves further investigation.

The comparison of the disagreement indices R obtained in the two cases is certainly of scarce significance. First, traditional R index is usually evaluated as $\sum|F_{obsd} - F_{calcd}|/\sum|F_{obsd}|$, while in our case it is based on intensities (proportional to F^2). Second, in the full-pattern case the sum is extended also over film regions far from the Bragg positions. Moreover, in the full-pattern case $I_{obsd} - I_{calcd}$ differences *evaluated point-by-point* may be greatly influenced not only by errors in structural quantities but also by errors in unit-cell and profile parameters and by specimen misalignment.

Acknowledgment. The financial support by Ministero della Pubblica Istruzione and by Consiglio Nazionale delle Ricerche (Strategic project on advanced crystallographic methods) is acknowledged.

Registry No. PIB, 9003-27-4.

References and Notes

(1) Iannelli, P.; Immirzi, A. *Macromolecules*, preceding paper in this issue.
(2) Immirzi, A.; Iannelli, P. *Gazz. Chim. Ital.* **1987**, *117*, 201.
(3) Immirzi, A.; Iannelli, P. *Macromolecules* **1988**, *21*, 768.
(4) Arnott, S.; Wonacott, A. J. *Polymer* **1966**, *7*, 157.
(5) Tanaka, T.; Chatani, Y.; Tadokoro, H. *J. Polym. Sci., Polym. Phys. Ed.* **1974**, *12*, 112.
(6) Tadokoro, H. *Structure of Crystalline Polymers*; Wiley: New York, 1979.
(7) Benedetti, E.; Pedone, C.; Allegra, G. *Macromolecules* **1970**, *3*, 16.
(8) Johnson, C. K. In *Crystallographic Computing*; Ahmed, F. H., Ed.; Munksgaard: Copenhagen, 1970, pp 220–226.
(9) Allegra, G.; Benedetti, E.; Pedone, C. *Macromolecules* **1970**, *3*, 727.
(10) Cooper, M. J. *Acta Crystallogr., Sect. A: Found. Crystallogr.* **1982**, *A38*, 264.
(11) Cooper, M. S.; Rouse, K. D.; Sakata, M. *Z. Kristallogr.* **1981**, *157*, 101.

Structural Studies of Polymers with Hydrophilic Spacer Groups: Infrared Spectroscopy of Langmuir–Blodgett Multilayers of Preformed Polymers with Hydrocarbon Side Chains

J. Schneider and H. Ringsdorf

University of Mainz, D-6500 Mainz, FRG

J. F. Rabolt*

IBM Research Division, Almaden Research Center, 650 Harry Road, San Jose, California 95120-6099.

Received March 21, 1988

ABSTRACT: A series of preformed polymers containing amphiphilic side chains and hydrophilic spacer groups in the backbone have been investigated by grazing incidence reflection and transmission infrared spectroscopy. In the former the electric field vector is normal to the film surface whereas in the latter, it is parallel to the surface. The two measurements taken collectively have provided information about the orientation of the ordered amphiphilic side groups and the partially disordered polymer backbone. The results indicate that there is a definite preferred orientation of the side chain axis normal to the substrate surface. The extent of this side chain order is affected by both the concentration of backbone spacer groups and the temperature of the Langmuir–Blodgett (LB) layers. These effects on the long-term aging of these polymeric multilayers will be discussed.

Introduction

It has long been recognized that thin films formed by Langmuir–Blodgett (LB) deposition offer an enticing alternative to films formed by conventional processing techniques.[1,2] In addition to being exceptionally thin (~25 Å) due to their molecular length, LB films can be molecularly designed so as to include functional chromophores within the individual layers.[3] Initially, many IR studies of LB multilayers[4–7] were focused on the assembly of fatty acid molecules on the water surface since closely packed stable structures could be formed and subsequently transferred to solid substrates. These investigations concentrated on determining order and orientation of cadmium arachidate,[6,7] $[C_{19}H_{39}COO^-]_2Cd^{2+}$, monolayers and multilayers transferred to reflective and transmissive substrates. Although this fatty acid was ideally suited for structural studies because of its high degree of order, it has been known for some time that multilayers do not have mechanical integrity and when submitted to aggressive environments (e.g., temperature and moisture), they undergo irreversible degradation.[8,9]

An attractive alternative was to incorporate within the amphiphilic molecules, reactive groups which could be polymerized by UV irradiation either on the water surface or on a solid substrate[10–13] in order to stabilize the films and provide mechanical strength. Unfortunately, contraction due to polymerization can lead to the creation of cracks and fissures[14–17] in the film, a trait undesirable especially if these films were to act as a diffusion barrier or insulating layer. In order to avoid this complication, recent interest has turned to the study of LB films of preformed polymers.[17] Initially, preformed homopolymers were investigated in order to assess the extent of molecular orientation and order. Tredgold and Winter[18] were the first to describe the deposition of LB monolayers of copolymers which first had to be hydrolyzed on the surface of the water subphase before transfer.

Recently, single monolayers of poly(octadecylmethacrylate) and poly(octadecylacrylate) (see Figure 1) were characterized by IR spectroscopy.[19] Dichroic studies indicated a preferential orientation of the *n*-alkyl side chains toward the surface normal with a loose intermolecular packing in the lattice. One possible reason for this lack of high orientation and order of the side chains can be attributed to their reduced mobility due to the stiffness of the polymer backbone. This particular problem has been addressed by Elbert et al.[17] with the incorporation of hydrophilic spacer groups into preformed polymers in order to increase the mobility of the monolayer. As a result, this reduced viscosity of the film promotes better self-organization of the amphiphilic side chains, therefore enhancing deposition behavior and multilayer quality.

It is the purpose of this work to report an IR study of a homopolymer and a series of related copolymers which contain amphiphilic side chains and various amounts of hydrophilic spacer group in the backbone[20] (see Figure 1). IR dichroic measurements have been made and utilized to determine the orientation of molecular groups in both the crystalline and amorphous components of the LB monolayers. The net result of incorporating hydrophilic spacer groups into the backbone on the molecular flexibility was investigated at room and elevated temperatures. This provided an assessment of the physical aging behavior[9] of these LB films which could then be compared

0024-9297/89/2222-0205$01.50/0